THE UNIVERSITY OF
WARWICK

University of Warwick institutional repository: http://go.warwick.ac.uk/wrap

This paper is made available online in accordance with
publisher policies. Please scroll down to view the document
itself. Please refer to the repository record for this item and our
policy information available from the repository home page for
further information.

To see the final version of this paper please visit the publisher's website.
Access to the published version may require a subscription.

Author(s): Oleg Palygin, Ulyana Lalo, Yuriy Pankratov
Article Title: Distinct pharmacological and functional properties of
NMDA receptors in mouse cortical astrocytes
Year of publication: 2011
Link to published article:
http://dx.doi.org/10.1111/j.1476-5381.2011.01374.x
Publisher statement: The definitive version is available at
www.interscience.wiley.com

Distinct pharmacological and functional properties of NMDA receptors in mouse cortical astrocytes.

Abbreviated title: Pharmacology of astroglial NMDARs

Oleg Palygin[1] , Ulyana Lalo[2] and Yuriy Pankratov[1].

[1]*Department of Biological Sciences, University of Warwick, Coventry, CV4 7AL, UK*
[2]*Cell Physiology and Pharmacology, University of Leicester, Leicester LE1 9HN, UK*

Address for correspondence:

Dr Yuriy Pankratov
Department of Biological Sciences
University of Warwick
Coventry, CV4 7AL, UK
Tel: +44 2476 528373
Fax: +44 2476 523568
e-mail: y.pankratov@warwick.ac.uk

Summary

Background and purpose

Astrocytes of the mouse neocortex express functional NMDA receptors which are not blocked by Mg^{2+}ions. However, study of the pharmacological profile of glial NMDARs and their subunit composition is far from complete.

Experimental approach

In the present study we tested the sensitivity of NMDA receptor-mediated currents in the cortical astrocytes and neurons to the novel GluN2C/D subunit-selective antagonist UBP141. We also examined the action of memantine, an antagonist reported to have substantially different affinities for GluN2A/B and GluN2C/D-containing receptors in physiological concentrations of extracellular Mg^{2+}.

Key results

UBP141 had a strong inhibitory action on NMDA receptor-mediated transmembrane currents in the cortical layer II/III astrocytes with an IC_{50} of 2.29 μM and a modest inhibitory action on NMDA-responses in the pyramidal neurons with IC_{50} of 19.8 μM. Astroglial and neuronal NMDA receptors exhibited different sensitivities to memantine with corresponding IC_{50} of 2.19 and 10.8 μM, respectively.

Consistent with pharmacological differences between astroglial and neuronal NMDA receptors, NMDA receptors in astrocytes showed lower Ca^{2+}-permeability than neuronal ones with P_{Ca}/P_{Na} ratio of 3.4.

Conclusions and Implications

The combination of biophysical and pharmacological properties of astrocytic NMDA receptors strongly suggests they have tri-heteromeric structure composed of GluN1, GluN2C/D and GluN3 subunits. Dramatic difference between astroglial and neuronal NMDA receptors in their sensitivity to UBP141 and memantine may enable selective modulation of astrocytic signalling that could be very helpful for

elucidating the mechanisms of neuron-glia communications. Our results may also provide a clue for development novel therapeutic agents specifically targeting glial signalling.

Keywords: Memantine; UBP141; NMDA receptor; GluN3A subunit; calcium permeability; neuron-glia communication; GluN3B; mouse cortex.

Introduction

N-methyl-D-aspartate receptors (NMDARs) are the most complex glutamate-gated ionotropic receptor in the CNS. They play a key role in the excitatory synaptic transmission and many brain functions, such as memory and cognition. Because of their involvement in various brain pathologies, including ischemia, neurodegenerative and neuropsychiatric disorders, NMDA receptors attract a great deal of interest in therapeutic research (Lipton, 2006; Paoletti and Neyton, 2007).

There is a great diversity in the NMDAR subtypes. It is widely accepted that functional NMDARs are tetrameric complexes assembled of the two obligatory GluN1 subunits combined with one or two GluN2(A,B,CD) and/or GluN3(A,B) subunits (Matsuda et al., 2003; Furukawa et al., 2005; Paoletti and Neyton, 2007). Subunit composition determines specific pharmacological and biophysical properties of NMDARs such as glutamate affinity, receptor desensitization, pharmacological sensitivity, and channel block by extracellular Mg^{2+} (Cull-Candy and Leszkiewicz, 2004; Paoletti and Neyton, 2007). GluN2 and GluN3 subunit expression exhibits regional specificity and undergoes developmental regulation (Monyer *et al.*, 1994; Cull-Candy and Leszkiewicz, 2004; Paoletti and Neyton, 2007; Henson 2010).

Until recently, attention has been focused on the role of NMDARs in neuronal function. The functional expression of NMDA receptors in glia was unappreciated for a long time. Because of the voltage-dependent Mg^{2+}-block, NMDA receptors were expected to be inactive at physiological resting potential in non-excitable glial cells. It has been reported only recently that glial cells, namely oligodendrocytes (Karadottir *et al.*, 2005; Micu *et al.*, 2006) and cortical astrocytes (Lalo *et el*., 2006), express functional NMDA receptors that have distinct biophysical properties and may be composed of subunits different from GluN2A and GluN2B. Most importantly, glial NMDARs exhibit the weak Mg^{2+}-block at physiological concentrations (Karadottir *et al*., 2005; Lalo *et al.* 2006) and therefore can be

active even at resting membrane potential. We have previously shown that astroglial NMDA receptors mediate transmembrane currents in cortical astrocytes activated upon physiological synaptic transmission (Lalo *et el.,* 2006).

Recent studies linking glial NMDARs to various neurological disorders ignited an interest in them as promising targets for the development of new therapeutic agents (Lipton, 2006; Matute *et al.,* 2006). Finding specific antagonists of astroglial NMDAR receptors could allow the selective modulation of astroglial signaling without directly affecting neurons. This would be very useful for the investigation of the mechanisms of astroglial modulation of synaptic transmission and plasticity. However, study of the pharmacological profile of glial NMDARs is far from complete.

We tested the sensitivity of astroglial NMDARs to the novel antagonist UBP141 reportedly exhibiting selectivity over different GluN2 subunits (Morley *et al*., 2005; Brothwell *et al.*, 2008). We also tested the action of memantine – a therapeutically used antagonist which was reported to have substantially different affinity for GluN2A/B and GluN2C/D-containing receptors in physiological concentrations of extracellular Mg^{2+} (Kotermanski and Johnson, 2009).

Methods

Slice and cell preparation

Experiments were performed on transgenic mice expressing enhanced green fluorescent protein (EGFP) under the control of the human glial fibrillary acidic protein (GFAP) promoter (line TgN(GFAP-EGFP)GFEC-FKi; see Nolte *et al*., 2001; Lalo *et al.*, 2006). Mice (4 - 8 weeks old) were anaesthetized by halothane (1.5-1.8 vol %) and then decapitated, in accordance with UK legislation. Slices were prepared using the technique described previously (Lalo *et al.*, 2006). Brains were rapidly dissected in physiological saline containing (in mM): 135 NaCl, 3 KCl, 3 $MgCl_2$, 0.5 $CaCl_2$, 26 $NaHCO_3$, 1 NaH_2PO_4, 15 glucose, pH 7.4 when gassed with

95% O_2 / 5%CO_2. Brain slices (280 - 300 µm thick) were cut at 4^{o} C and kept at room temperature for 1 - 4 h prior to *in situ* recordings and cell isolation in the above solution but with (mM) $CaCl_2$ 2.5 , $MgCl_2$ 1. The same extracellular solution was used for recordings in slices.

Astrocytes and neurons were acutely isolated from somatosensory cortex layer II/III using the modified "vibrating ball" technique (Pankratov *et al.*, 2002; Lalo *et al.*, 2006). The glass ball (200 µm diameter) was moved slowly some 10 - 50 µm above the slice surface, while vibrating at 100 Hz (lateral displacements 20 - 30 µm). The composition of external solution for isolated cell experiments was (mM): 135 NaCl; 2.7 KCl; 2 $CaCl_2$; 1 $MgCl_2$; 10 HEPES, 1 NaH_2PO_4, 15 glucose, pH adjusted with NaOH to 7.3. In some experiments, the extracellular $CaCl_2$ concentration was elevated to 20 mM.

Electrophysiology

Cells were initially identified by size and the shape of somata under IR gradient contrast and green fluorescence (astrocytes). After establishing the whole-cell recording configuration, identification of cells was verified by their response to a series of depolarizing and hyperpolarizing voltage steps from a holding potential of -80 mV (Lalo *et al.*, 2006). All cells identified visually by EGFP fluorescence demonstrated an electrophysiological signature characteristic of astrocytes, i.e series of passive currents with nearly linear I-V relationship, whereas cells identified as pyramidal neurons exhibited prominent rapidly-activating currents elicited by depolarization as described previously in (Lalo *et al.*, 2006).

Whole-cell voltage clamp recordings from the cortical astrocytes and pyramidal neurons were made with patch pipettes (5 - 6 MΩ) filled with intracellular solution (in mM): 110 KCl, 12 NaCl, 10 HEPES, 5 MgATP, 0.2 EGTA, pH 7.35. The membrane potential was clamped at -80 mV in the astrocytes and at -40 mV in the neurons unless stated otherwise. Currents were monitored using an AxoPatch200B patch-clamp amplifier (Axon Instruments) filtered at 2 kHz and digitized at 4 kHz. Experiments were controlled

by PCI-6229 data acquisition board (National Instruments) and WinFluor software (Strathclyde Electrophysiology Software); data were analyzed by custom-designed software.

Liquid junction potentials were measured with the patch-clamp amplifier; all voltages reported were corrected accordingly. Series resistances were 5-12 MΩ and input resistances were 50-150 MΩ for astrocytes and 400-900 MΩ for neurons; both varied by less than 20% in the cells accepted for analysis. A modified "square-pulse" concentration jump method (Pankratov *et al.,* 2002; Lalo *et al.,* 2006) was used for rapid applications of solutions containing various agents to the acutely isolated cells. Unless stated otherwise, transmembrane currents were evoked in acutely isolated cortical neurons and astrocytes by application of 50 μM NMDA and 1μM glycine. Antagonists of NMDA receptors were pre-applied for 2 min before application of agonist. Between agonist applications, cells were constantly perfused with agonist-free extracellular solution using gravity-fed bath application (flow rate 1-1.5 ml min^{-1}). Responses of the cortical neurons and astrocytes to glycine were recorded in presence of 10 μM strychnine and 100 μM picrotoxin.

To examine the synaptic currents *in situ*, voltage-clamp recordings were made from identified astrocytes and pyramidal neurons situated in the somatosensory cortex layer II/III at temperature of 30-32^{0}C. Axons originating from layer IV-VI neurones were stimulated at 0.15 Hz with a bipolar coaxial electrode (WPI, USA) placed in the layer IV approximately opposite the site of recording. Stimuli were single pulses (300 μs) of magnitude adjusted to produce a synaptic current in neurons that was 30-40% of the maximal response (typically, stimulus amplitude was 5–7 μA). At such stimulus strength the amplitude of response in the astrocytes reached 25-30% of maximal.

To isolate the NMDA receptor-mediated components of glial and neuronal currents activated by synaptic stimulation, cortical slices were treated with the following pharmacological agents: picrotoxin 100 µM, a combination of the inhibitors of glutamate transporters (Danbolt, 2001; Hu *et al*., 2003) (3S)-3-4-(Trifluoromethyl)benzoyl]amino]phenyl]methoxy-L-aspartic acid (TFB-TBOA), 1 µM and DL-threo-b-Benzyloxyaspartic acid (DL-TBOA), 30 µM; an antagonist of AMPA receptors, 6-Cyano-7-nitroquinoxaline-2,3-dione (CNQX), 50 µM; the P2X receptor antagonist pyridoxalphosphate-6-azophenyl-2',4'-disulfonic acid tetrasodium salt (PPADS), 30 µM. According to our previous reports (Lalo, *et al.* 2006; Lalo *et al.,* 2008) these concentrations of antagonists effectively inhibited P2X, AMPA receptors and glutamate transporters expressed in the cortical astrocytes and neurons.

Fluorescent Ca^{2+}-imaging

To monitor intracellular Ca^{2+}, cortical astrocytes were loaded with 150 µM Fluo-3 through the whole-cell patch-pipette (substituting the EGTA in the intracellular saline). Cells were illuminated at 495 nm using the OptoScan monochromator (Cairn, UK), fluorescence was measured at 530±20 nm.

The fluorescent images were recorded using an Olympus BX51 microscope with an UMPLFL20X/NA0.95 objective and 2X intermediate magnification and an iXon885 EMCCD camera (Andor Technology, UK); exposure time was 35 ms at 2X2 binning. Elevation in the intracellular Ca^{2+} level was evaluated by $\Delta F/F_0$ ratio after background subtraction.

Data analysis

Data on the concentration-dependence of the effects of antagonists were fitted with the following:

$I/I_0 = 1/(1+([B]/IC_{50})^p)$, where I is the current measured with drug concentration $[B]$, I_0 is the current in control conditions, and p is a Hill coefficient. The relative calcium permeability of NMDA receptors was calculated from the reversal potential of NMDA-activated current in the context of the extended Goldman-Hodgkin-Katz theory as described previously (Lewis 1979; Mayer and Westbrook, 1987;

Pankratov *et al.*, 2002). Briefly, the current-voltage relationships of NMDA-response were normalised to the amplitude at -40 mV, averaged over all cells and fitted with a polynomial curve to determine a reversal potential. The permeability ratios for Ca^{2+} to Na^{+} (P_{Ca}/P_{Na}) and Na^{+} to K^{+} (P_{Na}/P_{K}) were calculated from values of reversal potential at two different extracellular calcium concentrations converted to the activities in the electrolyte solutions (Mayer and Westbrook, 1987; Castro and Albuquerque, 1995); the following activity coefficients were used: 0.77 for Na^{+} and K^{+}, 0.29 and 0.26 for low and high concentrations of Ca^{2+}.

Drugs

UBP141 was purchased from Ascent Scientific (UK), other receptor antagonists were from the Tocris Bioscience, other salts and chemicals were from Sigma (Dorset, UK).

Results

Agonist-evoked currents in acutely isolated astrocytes and neurons

Recordings from visually-identified acutely isolated fluorescent astrocytes were made within 20–50 min after isolation. Taking into account the competitive mechanism of UBP141 action (Morley et al., 2005) we activated astrocytic NMDA receptors by saturating concentration of NMDA (50µM, see Lalo *et al.,* 2006; Erreger et al., 2007). Application of 50 µM NMDA with 1µM glycine at a holding potential -80 mV (in 1 mM extracellular Mg^{2+}) evoked inward currents in all of 58 astrocytes tested (Fig.1A). Functional properties of NMDA-activated currents, i.e slow desensitization kinetics, high affinity to agonist, sensitivity to D-AP5 and lack of Mg^{2+} block were similar to our data reported previously for cortical astrocytes (Lalo *et al*., 2006, see also Fig.4A). Contrary to the astrocytes, L2/3 pyramidal neurons did not respond to NMDA at holding potential of –80 mV due to Mg^{2+}-block; currents elicited by NMDA in the

pyramidal neurons at other holding potentials had functional properties very similar to NMDA receptors in hippocampal and cortical neurons (Mayer and Westbrook, 1987; Lalo *et al*.,2006, see also Fig.4B). Unless stated otherwise, all experiments reported below were carried out at holding potential -80 mV in astrocytes and at -40 mV in neurons.

UBP141, novel subunit-selective antagonist of NMDA receptors, had different inhibitory action in astrocytes and neurons (Fig.1). Pre-incubation with 3 μM UBP141 for 2 min decreased the amplitude of NMDA-evoked responses (Fig.1A) in the astrocytes by 62 ± 14% (n=7) whereas neuronal responses (Fig.1B) were inhibited by only 9±11% (n=6). The action of UBP141 was reversible in both astrocytes and neurons. The inhibitory action of UBP141 on NMDA-activated currents in cortical astrocytes was concentration-dependent (Fig.1C) with an IC_{50} of 2.29±0.37 μM (n=7). The IC_{50} for glial NMDARs was close to IC_{50} values reported for the action of UBP141 on GluN1/GluN2C- and GluN1/GluN2D receptor-mediated responses activated by saturating concentration of agonist (Morley *et al*., 2005). The IC_{50} for the effect of UBP141 on NMDA-responses recorded in neurons was 19.8±3.4 μM (n=6); this value closely agrees with IC_{50} values for GluN1/GluN2A and GluN1/GluN2B receptors (Morley *et al*., 2005).

We also tested the inhibitory action of another subunit-selective NMDAR antagonist – ifenprodil. Incubation with 10 μM ifenprodil did not significantly affect the amplitude of NMDA-activated currents in the cortical astrocytes (3±7% decrease; n=15, $P > 0.05$, one-population t-test; data not shown). In contrast, the same concentration of ifenprodil inhibited the NMDA-response in cortical neurons by 58±11% (n=6, data not shown). The absence of notable effect of ifenprodil on NMDA-response in the astrocytes indicates low level (if any) expression of GluN2B subunits. This result is slightly different from our previous data (Lalo *et al.* 2006) obtained in younger mice (17-22 day-old), where we observed partial (less than 50%) inhibition of NMDA receptors by 10 μM ifenprodil in the sub-population (about

30%) of cortical astrocytes. The expression of both GluN2B and GluN2C subunits in the mouse cortical astrocytes, also in younger age, has been reported by Schipke *et al.* (2001). The variation in the subunit composition of astroglial NMDARs may be related to developmental changes, like it happens in neurons where decrease in the expression of GluN2B and increase in the expression of GluN2C subunit have been reported (Henson *et al.* 2010; Steinert *et al.* 2010). Also, the pathologically evoked expression of GluN2B subunit might occur in the astrocytes in some cases after ischemic insults during tissue preparation, as it has been observed by (Krebs *et al*. 2003).

Dramatic difference in the inhibitory action of UBP141 suggests different subunit composition of NMDA receptors in cortical astrocytes and neurons, presumably lack of GluN2A and B subunits and incorporation of GluN2C or D subunits in astroglial NMDARs. This hypothesis was supported by data on the inhibitory action of memantine (Fig.2). Taking into account that action of memantine on NMDA receptors depends on membrane potential and extracellular Mg^{2+} concentration (Wrighton et al., 2008; Kotermanski and Johnson, 2009), we measured effect of memantine on astroglial and neuronal receptors at physiological Mg^{2+} concentrations and membrane potentials at which these receptors would likely be activated during physiological activity, correspondingly -80 mV and -40 mV. Pre-application of 1 μM and 10 μM memantine decreased the amplitude of NMDA-evoked currents in the astrocytes (Fig.2A) by 39 ± 12% and 72±7% respectively (n=7). However, neuronal responses to NMDA (Fig.2B) were correspondingly inhibited by 7±11% and 46±10% (n=6).

Memantine exhibited different affinities for glial and neuronal NMDA receptors (Fig. 2C). The IC_{50} for the action of memantine on NMDA-evoked currents in the cortical astrocytes was 2.19±0.18 μM (n=7) at -80 mV and 4.24±0.47 μM (n=5) at -40 mV. The weak voltage-dependence of the effect of memantine on astroglial NMDA receptors was similar to the voltage-dependence of memantine action on GluN2D receptors (Wrighton et al., 2008). The IC_{50} for the action of memantine on NMDA receptors in the

cortical neurons was 10.8±0.55 μM (n=6) at -40 mV. It should be emphasized that the IC_{50} value for NMDA-evoked currents in neurons obtained in our experiments is in very good agreement with the data of Kotermanski and Johnson (2009) on the affinity of memantine to GluN2A and B subunits (constituent subunits of the majority of neuronal NMDARs) in physiological concentrations of Mg^{2+}. At the same time, the IC_{50} for the action of memantine on NMDA-responses in astrocytes closely agrees with the sensitivity of GluN2C/D-containing receptors (Kotermanski and Johnson, 2009).

Synaptically-activated currents in cortical astrocytes and neurons in situ

Results obtained in the acutely-isolated cells were corroborated by data on the pharmacological sensitivity of NMDA receptor-mediated components of synaptic response in astrocytes and neurons in brain slices. We performed voltage-clamp recordings from protoplasmic astrocytes and pyramidal neurons in layer II/III of somato-sensory cortex of EGFP/GFAP mice (Nolte *et al*., 2001). The astrocytes in acutely prepared brain slices were identified by green fluorescence and by their characteristic electrophysiological signatures (see *Methods*).

Stimulation of neuronal afferents originating from layers IV-VI in presence of 100 μM picrotoxin induced excitatory postsynaptic currents (EPSCs) in neurons and transmembrane ion currents in the astrocytes (Fig.3, see also Lalo *et al*., 2006). Ion currents induced in the astrocytes were directly associated with synaptic transmission because (i) treatment of slices with 1 μM TTX completely abolished glial responses, (ii) the amplitude of the glial response was stimulus-dependent in a manner similar to the synaptic current evoked in the neighboring neurons and (iii) latency time of glial responses was the same as latency of EPSCs (1.5-2.5 ms). Therefore, we identified astroglial responses as glial synaptic currents (GSCs). As it has been shown before (Lalo *et al.,* 2006), the major part of cortical GSC is

mediated by glial NMDA receptors and glutamate transporters. Also, AMPA and P2X receptors can participate in ionotropic signaling in cortical astrocytes (Lalo *et al.,* 2006, Lalo *et al.,* 2008). As we have discussed previously (Lalo *et al.,* 2006), astrocytic GSCs most likely result from both spill-out of neurotransmitter from cortical synapses and ectopic release similarly to Bergmann glial cells (Matsui and Jahr, 2004). Cortical astrocytes may also be a direct target of axon collaterals, like NG2+ glial cells in hippocampus and cerebellum (Bergles *et al.*, 2009).

To isolate NMDA receptor-mediated synaptic responses, recordings were carried out in presence of CNQX (30μM), TFB-TBOA (1μM), DL-TBOA (30 μM) and PPADS (30μM). GSCs recorded under these conditions in astrocytes at -80 mV had 10-90% rise time of 19.3±4.2 ms and decay time of 690±210 ms (n=22); corresponding parameters of EPSCs recorded in neurons at -40 mV were 8.9±2.7 ms and 148±41 ms (n=22). Application of 30 μM D-AP5 inhibited the astrocytic GSCs and neuronal EPSCs correspondingly by 96±7% and 93±9% (n=5, data not shown).

Similar to NMDA-activated currents in the acutely isolated cells, NMDA receptor-mediated synaptic responses in astrocytes and neurons *in situ* exhibited different sensitivity to UBP141, ifenprodil and memantine (Fig.3). Application of 3 μM UBP141 to cortical slices decreased the amplitude of astrocytic GSCs by 58±6% (n=9), which recovered after washout of UBP141. However, consecutive application of ifenprodil (10 μM) did not cause notable effect on astrocytic NMDA receptors (Fig.3A). In contrast, application of 3 μM UBP141 decreased the amplitude of neuronal EPSCs only by 8±6% whereas ifenprodil inhibited EPSCs by 63±9% (n=9).

Application of memantine confirmed the differential sensitivity of astrocytic and neuronal response to NMDA. Memantine (1 μM and 10μM; Fig.3B) reversibly inhibited astrocytic GSCs by 41±8% and 81±6%

respectively (n=8). However, 1 μM memantine had no effect on neuronal EPSCs (inhibition by 5±6%; P > 0.05, one-population t-test), whilst the 10 μM memantine inhibited EPSCs by 49±8% (n=8).

Theoretically, changes in the extracellular potassium concentration due to activity of neuronal glutamate receptors might contribute to the inward current activated in the astrocytes by stimulation of synaptic pathways. To verify that decrease in the GSCs amplitude observed in the above experiments originated inhibition of astrocytic NMDA receptors, we perfused cortical astrocytes with 10 μM MK801 through the patch-pipette and applied D-AP5, UBP141 and memantine in the bath solution. Blocking of astrocytic NMDA receptors with intracellular MK-801 caused slow but strong inhibition of GSC recorded in presence of 100 μM picrotoxin, 50 μM CNQX and 30 μM PPADS in all 10 cells tested (Fig.3C). Neither D-AP5 nor UBP141 had notable effect (n=6) on the residual GSCs resistant to intracellular MK-801; this residual current was almost completely abolished after application of glutamate transporter blockers TFB-TBOA (1 μM) and DL-TBOA(30 μM). Similarly, memantine (10 μM) did not exhibit inhibitory action on GSCs in presence of intracellular MK801 in all 4 astrocytes tested (data not shown).

These results confirm that action of UBP141 and memantine was due to direct inhibition of astrocytic NMDA receptors. The small residual GSC (2±4%, n=10) remaining in presence of antagonists of NMDA receptors and glutamate transporters may, however, be associated with redistribution of the extracellular potassium in the vicinity of the astroglial membrane.

It is worth to note that inhibitory effects of UBP141 and memantine observed in astrocytes and neurons *in situ* closely agree with data obtained in acutely isolated cells. Importantly, our results demonstrate the feasibility of selective pharmacological modulation of NMDA receptor-mediated signalling in neurons and astrocytes in physiological conditions.

Functional properties and subunit composition of astroglial NMDARs

The above results suggest incorporation of GluN2C/D subunits in NMDA receptors expressed in cortical astrocytes. Although GluN2C/D subunits have low affinity to Mg^{2+} than GluN2A/B, they are still blocked by physiological concentrations (>0.5 mM) of Mg^{2+} (Qian and Johnson, 2006). In contrast, NMDARs containing one or two GluN3 subunits were shown to have much lower sensitivity to Mg^{2+}-block at physiological concentrations (Sasaki *et al*. 2002; Tong *et al.* 2008; Henson *et al.*, 2010). Incorporation of GluN3 subunits, however, renders much lower calcium permeability to the NMDARs.

Taking into account the importance of Ca^{2+}-signalling for the physiological activity of glial cells, we evaluated Ca^{2+}-permeability of astroglial NMDARs using the Goldman-Hodgkin-Katz theory (see Methods). The reversal potential of NMDA-induced currents in the isolated cortical astrocytes in 2 and 20 mM extracellular Ca^{2+} was 0.92±0.89 mV and 7.5±2.4 mV (n=7) respectively (Fig.4). The corresponding values for the neuronal NMDA-responses were 2.75±0.97 mV and 14.1±2.8 mV (n=6). The permeability ratio P_{Ca}/P_{Na} calculated from the reversal potential of NMDA-mediated current was 3.4 for astrocytes and 7.5 for neurons.

The obtained P_{Ca}/P_{Na} ratio for the NMDARs in cortical neurons agrees with data reported previously for neuronal NMDARs and various heterologously expressed GluN1/GluN2 subunit combinations (Mayer and Westbrook, 1987; Lino *et al.,* 1990; Matsuda *et al.,* 2003; Tong *et al.,* 2008). On the other hand, our evaluation of the relative Ca^{2+}-permeability of astroglial NMDARs is very close to the results of recent studies of GluN3 subunit-containing receptors (Sasaki *et al*., 2002; Matsuda *et al.,* 2003; Tong *et al.,* 2008). It should be emphasized that even though the Ca^{2+}-permeability of astroglial NMDA receptors is lower compared to neuronal NMDARs, it is close to the permeability of other ionotropic receptors, like neuronal nicotinic ACh receptors (P_{Ca}/P_{Na}≈2.1-6.1) or P2X1 (P_{Ca}/P_{Na} =3.9) and P2X2 (P_{Ca}/P_{Na} =2.2)

receptors (Castro and Albuquerque, 1995; Evans *et al.,* 1996; Fucile 2004) and is larger than the permeability of Ca^{2+}-permeable kainate (P_{Ca}/P_{Na}=0.74) and AMPA (P_{Ca}/P_{Na}≈0.5-1.7) receptors (Burnashev *et al.*, 1996; Isa *et al.*, 1996).

To verify that astroglial NMDA receptors can contribute to Ca^{2+}-signalling, we measured elevation in the cytosolic Ca^{2+} level simultaneously with transmembrane currents induced by application of glutamate and NMDA to the isolated cortical astrocytes (Fig.5). Both NMDA and glutamate triggered significant rise in the intracellular Ca^{2+} in the astrocytes. Amplitude of NMDA-induced Ca^{2+}-transients reached 56.8±13.1 % (n=5) of Ca^{2+}-transients activated by glutamate whereas amplitudes of NMDA-activated and glutamate-activated transmembrane currents were almost similar. Application of 30 μM D-AP5 decreased the magnitude glutamate-activated Ca^{2+}-transients (Fig.5) by 54.1±10.9% (n=5) and inhibited transmembrane current even strongly (89.4±12.3%, n=5); transmembrane currents were eliminated by further application of 30 μM NBQX (data not shown). These observations clearly indicate that substantial component of glutamatergic Ca^{2+}-signalling in cortical astrocytes is independent of NMDA receptors. This component is most likely mediated by metabotropic glutamate receptors whose participation in the astroglial Ca^{2+}-signalling has been widely reported (Agulhon *et al.* 2008). Our data also show that astroglial NMDARs, by virtue of their Ca^{2+}-permeability and weak Mg^{2+}-block, are capable of delivering significant Ca^{2+}-influx in cortical astrocytes. One could estimate the contribution of NMDA receptors to the Ca^{2+}-transients elicited by glutamate as 50-55%.

The combination of the lack of Mg^{2+}-block together with lower Ca^{2+}-permeability strongly suggests the presence of the GluN3 subunit in glial NMDARs. Accordingly, the expression of pure di-heteromeric GluN1/GluN3 receptors in cortical astrocytes cannot be ruled out a priori. The most characteristic property of such receptors is a capability to be activated by application of glycine or D-serine in the absence of glutamate. We found that glycine and D-serine acted as weak agonists, inducing inward

currents of much smaller amplitude than currents induced by NMDA or glutamate, in all 10 astrocytes tested (Fig.6). This contrasts with the much higher potency of glycine that one would expect of pure GluN1/GluN3 receptors (Chatterton *et al.*, 2002; Henson *et al.,* 2010). We also observed potentiation of NMDA-activated currents in astrocytes by 10 µM D-serine (Fig.6), this is in contrast to the D-serine-induced desensitization of GluN1/GluN3 receptors reported previously (Chatterton *et al.*, 2002). On the other hand, partial agonistic action of glycine in the cortical astrocytes closely agrees with data reported for GluN1/ GluN2A/GluN3B tri-heteromeric receptors (Cavara and Hollmann, 2008).

To elucidate whether currents activated in the cortical astrocytes by glycine and D-serine were mediated by di-heteromeric or tri-heteromeric receptors, we tested their sensitivity to NMDA receptor antagonists. Weak block by classic NMDA antagonists is a characteristic feature of GluN1/GluN3 receptors whereas triplet GluN1/GluN2/GluN3 receptors can be blocked by antagonists targeting GluN2 subunits (Sasaki *et al.,* 2002; Smothers and Woodward, 2010; Henson *et al.* 2010). MK-801 (10 µM), memantine (10 µM) and UBP141 (10 µM) showed strong inhibitory action on the response of astrocytes to glycine (Fig.7A) and D-serine (Fig. 7B). Inhibitory effects NMDAR antagonists on glycine and D-serine-activated currents in the astrocytes did not differ significantly from their action on NMDA-activated currents (Fig. 7C) indicating that di-heteromeric GluN1/GluN3 receptors bring a little contribution to glutamatergic signalling in cortical astrocytes. Taken together, our results suggest that NMDA receptors in cortical astroglia are assembled from GluN1, GluN2 and GluN3 subunits.

Discussion

Our results demonstrate striking difference in the properties of astrocytic and neuronal NMDA receptors. Moreover, our findings provide several clues to identify the subunit composition of astroglial NMDARs. There is no doubt that glial NMDARs contain two GluN1 subunits that are essential for

trafficking to the membrane (Matsuda *et al.*, 2003; Furukawa *et al.*, 2005). In di- and tri-heteromeric NMDARs, expression of certain types of GluN2A-D subunits confers sensitivity to selective antagonists, such as D-AP5 or ifenprodi (Paoletti and Neyton, 2007). Hence, the most feasible explanation for the high affinity of astroglial receptors to UBP141 and memantine and their low sensitivity to ifenprodil is incorporation of GluN2C or GluN2D subunits. This hypothesis is also corroborated by very high potency of glutamate and NMDA to astroglial NMDARs to (Lalo *et al.,* 2006) which is close to the data reported for recombinant GluN1/GluN2D receptors (Erreger *et al.*, 2007).

At the same time, glial NMDA receptors have a very low sensitivity to Mg^{2+}-block, as has been shown already in (Lalo et al., 2006) and confirmed again in our present experiments. The only type of NMDA subunits, insensitive to Mg^{2+} in physiological concentrations is the GluN3 subunit. The stoichiometry of astroglial NMDARs might be different however, with incorporation of either one or two GluN3 subunits (Henson *et al*., 2010). The functional expression of GluN1/GluN3 di-heteromeric receptors has been suggested for cerebrocortical neurons (Chatterton *et al.*, 2002); white matter oligodendrocytes have been shown to express tri-heteromeric receptors (Karadottir *et al*., 2005; Burzomato *et al*. 2010).

The most peculiar feature of di-heteromeric GluN1/GluN3 receptors is their capability to be activated by glycine and, arguably, D-serine with higher potency than glutamate that even gave rise to the alternative term “excitatory glycine receptors” (Chatterton *et al.,* 2002). These properties do not agree with our observations: we did not observe a high potency of glycine and D-serine in the activation of inward currents in the cortical astrocytes (Fig.6). We observed potentiation of NMDA-activated currents by D-serine (Fig.6) not desensitization, which is not expected for GluN1/GluN3 assembly (Henson *et al.,* 2010). Furthermore, both NMDA-activated currents and responses to glycine and D-serine were strongly inhibited by D-AP5 (Lalo *et al.,* 2006), memantine (Fig.2,3) and MK-801 (Fig.4 and 7). Thus, the

pharmacological profile of NMDA-mediated responses in cortical astrocytes does not allow attributing them purely to di-heteromeric GluN1/GluN3 receptors.

The only structural composition that can explain all pharmacological and functional properties of the astroglial NMDARs we describe here is a tri-heteromer incorporating, in addition to two GluN1 subunits, one of GluN2C or D subunit and one GluN3 subunit, rendering astroglial receptors much less sensitive to Mg^{2+} but sensitive to UBP141, memantine and D-AP5 (Fig.1, 3 and 7). This suggestion is supported by the weak Mg^{2+}-block observed for tri-heteromeric GluN1/GluN2/GluN3 receptors (Sasaki *et al.,* 2002; Tong *et al*., 2008). It is also in line with evidence of expression of GluN2C, GluN2D and GluN3 subunits in white matter oligodendrocytes (Karadottir *et al*., 2005; Burzomato *et al.*, 2010).

It is worth to note that astroglial NMDARs showed lower sensitivity to Mg^{2+} -block than GluN1/GluN2C/GluN3A receptors in oligodendrocytes (Karadottir *et al*., 2005; Burzomato *et al.*, 2010). This might be explained by incorporation of different splice variants of GluN1 and GluN2 subunits and/or incorporation of GluN3B subunit. It has been shown that co-assembly of GluN3 with different splice variants of GluN1 subunit can affect functional properties of di-heteromeric receptors (Cavara *et al.*, 2009; Smothers and Woodward, 2009). In particular, fractions of glycine-activated currents blocked by Mg^{2+} in the receptor complexes assembled with GluN1-2b and GluN1-3b were much lower than in the receptors containing other GluN1 variants (Cavara *et al.*, 2009). Futhermore, degree of Mg^{2+} -block of almost all isoforms of GluN1/GluN3B receptors (Cavara *et al.*, 2009) was lower than Mg^{2+} -block reported for GluN1/GluN3A receptors (Chatterton *et al.,* 2002). It has also been reported recently that splicing of GluN2A subunit can lead to loss of Mg^{2+}-block (Endele *et al.*, 2010). Thus, one could speculate that co-assembly of GluN3A or GluN3B with different variants of GluN1 and GluN2 subunits might result in the tri-heteromeric receptors with different sensitivity to Mg^{2+}.

Whatever is the particular mechanism explaining the variance in the Mg^{2+}-sensitivity conferred by GluN3 subunits to glial triplet receptors, Mg^{2+}-sensitivity is weak both in astrocytes and oligodendrocytes. This may have similar physiological consequences: glial NMDARs can be activated at physiological resting potentials and bring significant contribution to glial Ca^{2+}-signalling despite their reduced Ca^{2+}-permeability. In view of possible implication of GluN3-containing receptors in brain injures (Henson et al., 2010), the molecular structure of glial NMDARs is worth further investigation.

The other important finding of the present study is the difference in the affinity of glial and neuronal NMDARs to memantine in physiological concentrations of Mg^{2+}. The recent successes of memantine in treatment of Alzheimer's disease revived interest in the therapeutic use of NMDA antagonists (Lipton, 2006). Our findings strongly support the conclusions of Kotermanski and Johnson (2009) that neuronal NMDARs can have much lower affinity to memantine in physiological conditions than was previously thought and that the clinical effects of therapeutic doses of memantine are most likely related to its action on GluN2C/D- rather than on GluN2A/B-containing receptors. Furthermore, our results suggest that those GluN2C and D subunits, which might underlie the therapeutic effects of memantine, may be mediated via astroglial NMDA receptors.

We have shown that the substantial difference in pharmacological and biophysical properties of astroglial and neuronal NMDARs enables the selective modulation of synaptically-driven astrocytic signalling. This may be very useful for elucidating the mechanisms of neuron-glia communications and development of novel therapeutic agents specifically targeting glial signalling.

Acknowledgements: This work was supported by a grant from BBSRC UK (BB/F021445; Y.P.).
The authors thank Prof. B. Frenguelli and Prof. N. Dale for early discussion and helpful comments on the manuscript.

References

Agulhon C, Petravicz J, McMullen AB, Sweger EJ, Minton SK, Taves SR, Casper KB, Fiacco TA, McCarthy KD (2008). What is the role of astrocyte calcium in neurophysiology? Neuron 59:932-946.

Bergles DE, Jabs R, Steinhauser C (2009). Neuron-glia synapses in the brain. Brain Res Rev 63:130-137.

Brothwell SL, Barber JL, Monaghan DT, Jane DE, Gibb AJ, Jones S (2008). NR2B- and NR2D-containing synaptic NMDA receptors in developing rat substantia nigra pars compacta dopaminergic neurones. J Physiol 586:739-750.

Burnashev N, Villarroel A Sakmann B (1996). Dimensions and ion selectivity of recombinant AMPA and kainate receptor channels and their dependence on Q/R site residues. J Physiol, London 496:165-173.

Burzomato V, Frugier G, Perez-Otano I, Kittler JT, Attwell D (2010). The receptor subunits generating NMDA receptor mediated currents in oligodendrocytes. J Physiol 588:3403-3414.

Cavara NA, Hollmann M (2008). Shuffling the deck anew: how NR3 tweaks NMDA receptor function. Mol Neurobiol 38:16-26.

Cavara NA, Orth A, Hollmann M (2009). Effects of NR1 splicing on NR1/NR3B-type excitatory glycine receptors. BMC Neurosci 10:32.

Castro NG, Albuquerque EX (1995). alpha-Bungarotoxin-sensitive hippocampal nicotinic receptor channel has a high calcium permeability. Biophys J 68:516-524.

Chatterton JE, Awobuluyi M, Premkumar LS, Takahashi H, Talantova M, Shin Y, Cui J, Tu S, Sevarino KA, Nakanishi N, Tong G, Lipton SA, Zhang D (2002). Excitatory glycine receptors containing the NR3 family of NMDA receptor subunits. Nature 415:793-798.

Cull-Candy SG, Leszkiewicz DN (2004). Role of distinct NMDA receptor subtypes at central synapses. Sci STKE 2004:re16.

Danbolt NC (2001). Glutamate uptake. Prog Neurobiol 65:1-105.

Endele S, Rosenberger G, Geider K, Popp B, Tamer C, Stefanova I, et al. (2010). Mutations in GRIN2A and GRIN2B encoding regulatory subunits of NMDA receptors cause variable neurodevelopmental phenotypes. Nat Genet 42:1021-1026.

Erreger K, Geballe MT, Kristensen A, Chen PE, Hansen KB, Lee CJ, et al. (2007). Subunit-specific agonist activity at NR2A-, NR2B-, NR2C-, and NR2D-containing N-methyl-D-aspartate glutamate receptors. Mol Pharmacol 72:907-920.

Evans RJ, Lewis C, Virginio C, Lundstrom K, Buell G, Surprenant A, North RA (1996). Ionic permeability of, and divalent cation effects on, two ATP-gated cation channels (P2X receptors) expressed in mammalian cells. J Physiol 497 (Pt 2):413-422.

Fucile S (2004). Ca2+ permeability of nicotinic acetylcholine receptors. Cell Calcium 35:1-8.

Furukawa H, Singh SK, Mancusso R, Gouaux E (2005). Subunit arrangement and function in NMDA receptors. Nature 438:185-192.

Henson MA, Roberts AC, Perez-Otano I, Philpot BD (2010). Influence of the NR3A subunit on NMDA receptor functions. Prog Neurobiol 91:23-37.

Hu WH, Walters WM, Xia XM, Karmally SA, Bethea JR (2003). Neuronal glutamate transporter EAAT4 is expressed in astrocytes. Glia 44:13-25.

Isa T, Itazawa S, Iino M, Tsuzuki K Ozawa S (1996). Distribution of neurones expressing inwardly rectifying and Ca^{2+}-permeable AMPA receptors in rat hippocampal slices. J Physiol, London 491:719-733.

Karadottir R, Cavelier P, Bergersen LH, Attwell D (2005). NMDA receptors are expressed in oligodendrocytes and activated in ischaemia. Nature 438:1162-1166.

Kotermanski SE, Johnson JW (2009). Mg2+ Imparts NMDA Receptor Subtype Selectivity to the Alzheimer's Drug Memantine. J Neurosci 29: 2774 –2779.

Lalo U, Pankratov Y, Kirchhoff F, North RA, Verkhratsky A (2006). NMDA receptors mediate neuron-to-glia signaling in mouse cortical astrocytes. J Neurosci 26:2673-2683.

Lalo U, Pankratov Y, Wichert SP, Rossner MJ, North RA, Kirchhoff F, Verkhratsky A (2008). P2X1 and P2X5 subunits form the functional P2X receptor in mouse cortical astrocytes. J Neurosci 28:5473-5480.

Lewis C.A. (1979) Ion-concentration dependence of the reversal potential and single cell conductance of ion channel at the frog neuromuscular junction. Journal of Physiology (Lond) 286: 417-445

Iino M, Ozawa S, Tsuzuki K (1990). Permeation of calcium through excitatory amino acid receptor channels in cultured rat hippocampal neurones. J Physiol 424:151-165.

Lipton SA (2006). NMDA receptors, glial cells, and clinical medicine. Neuron 50: 9-11.

Matsuda K, Fletcher M, Kamiya Y, Yuzaki M (2003). Specific assembly with the NMDA receptor 3B subunit controls surface expression and calcium permeability of NMDA receptors. J Neurosci 23:10064-10073.

Matsui K, Jahr CE (2004). Differential control of synaptic and ectopic vesicular release of glutamate. J Neurosci 24:8932-8939.

Matute C, Domercq M, Sanchez-Gomez MV (2006). Glutamate-mediated glial injury: mechanisms and clinical importance. Glia 53:212-224.

Mayer ML, Westbrook GL (1987). Permeation and block of N-methyl-D-aspartic acid receptor channels by divalent cations in mouse cultured central neurones. J Physiol 394:501-527.

Micu I, Jiang Q, Coderre E, Ridsdale A, Zhang L, Woulfe J, Yin X, Trapp BD, McRory JE, Rehak R, Zamponi GW, Wang W, Stys PK (2006). NMDA receptors mediate calcium accumulation in myelin during chemical ischaemia. Nature 439:988-992.

Monyer H, Burnashev N, Laurie DJ, Sakmann B, Seeburg PH (1994). Developmental and regional expression in the rat brain and functional properties of four NMDA receptors. Neuron 12: 529-540.

Morley RM, Tse HW, Feng B, Miller JC, Monaghan DT, Jane DE (2005). Synthesis and pharmacology of N1-substituted piperazine-2,3-dicarboxylic acid derivatives acting as NMDA receptor antagonists. J Med Chem 48:2627-2637.

Nolte C, Matyash M, Pivneva T, Schipke CG, Ohlemeyer C, Hanisch UK, Kirchhoff F, Kettenmann H (2001). GFAP promoter-controlled EGFP-expressing transgenic mice: a tool to visualize astrocytes and astrogliosis in living brain tissue. Glia 33:72-86.

Pankratov Y, Lalo U, Krishtal O, Verkhratsky A (2002). Ionotropic P2X purinoreceptors mediate synaptic transmission in rat pyramidal neurones of layer II/III of somato-sensory cortex. J Physiol 542:529-536.

Paoletti P, Neyton J (2007). NMDA receptor subunits: function and pharmacology. Curr Opin Pharmacol 7:39-47.

Qian A, Johnson JW (2006). Permeant ion effects on external Mg2+ block of NR1/2D NMDA receptors. J Neurosci 26:10899-10910.

Sasaki YF, Rothe T, Premkumar LS, Das S, Cui J, Talantova MV, Wong HK, Gong X, Chan SF, Zhang D, Nakanishi N, Sucher NJ, Lipton SA (2002). Characterization and comparison of the NR3A subunit of the NMDA receptor in recombinant systems and primary cortical neurons. J Neurophysiol 87:2052-2063.

Smothers CT, Woodward JJ (2009). Expression of glycine-activated diheteromeric NR1/NR3 receptors in human embryonic kidney 293 cells Is NR1 splice variant-dependent. J Pharmacol Exp Ther 331:975-984.

Steinert JR, Postlethwaite M, Jordan MD, Chernova T, Robinson SW, Forsythe (2010). NMDAR-mediated EPSCs are maintained and accelerate in time course during maturation of mouse and rat auditory brainstem in vitro. J Physiol 588:447-463.

Tong G, Takahashi H, Tu S, Shin Y, Talantova M, Zago W, Xia P, Nie Z, Goetz T, Zhang D, Lipton SA, Nakanishi N (2008). Modulation of NMDA receptor properties and synaptic transmission by the NR3A subunit in mouse hippocampal and cerebrocortical neurons. J Neurophysiol 99:122-132.

Wrighton DC, Baker EJ, Chen PE, Wyllie DJ (2008). Mg^{2+} and memantine block of rat recombinant NMDA receptors containing chimeric NR2A/2D subunits expressed in Xenopus laevis oocytes. J Physiol 586:211-225.

Legends for Figures

Figure 1

The NR2C/D subunit-selective antagonist UBP141 differentially suppresses NMDA receptors in the astrocytes and neurons. ***A***, Representative traces illustrate the current activated by 50 μM NMDA in the acutely isolated cortical layer II/III astrocyte before and after application of 3 and 10 μM of UBP141. ***B***, action of the same concentrations of UBP141 on current activated by 50 μM NMDA in a pyramidal neuron acutely isolated from the same cortical slice. Note much weaker inhibitory effect of UBP141 in the neuron. ***C***, the mean concentration-dependence of UBP141 action in 7 astrocytes (IC_{50}, 2.29±0.37 μM; Hill coefficient, 1.19±0.14) and 6 neurons (IC_{50}, 19.8±3.4 μM; Hill coefficient, 1.08±0.15). Amplitude of NMDA-response was normalized to control. Error bars represent SD. Holding membrane potential was -80 mV in astrocytes and -40 mV in neurons.

Figure 2

Memantine differentially inhibits NMDA receptors in astrocytes and neurons. ***A***, Representative traces illustrate the NMDA-activated current recorded in the acutely isolated cortical layer II/III astrocyte before and after application of 1 and 10 μM of memantine. ***B***, action of the same concentrations of memantine on NMDA-activated current in a pyramidal neuron acutely isolated from the same cortical slice. Note the much weaker inhibitory effect of memantine in the neuron. ***C***, the mean concentration-dependence of memantine action in 7 astrocytes at -80 mV (blue line, IC_{50}, 2.19±0.18 μM; Hill coefficient, 1.01±0.07), in 5 astrocytes at -40 mV (red line, IC_{50}, 4.24±0.47 μM; Hill coefficient, 1.03±0.11) and in 6 neurons at -40 mV (IC_{50}, 10.8±0.55 μM; Hill coefficient, 1.04±0.05). Error bars represent SD.

Figure 3.

Action of UBP141 and memantine on the NMDA-receptor mediated synaptic currents in astrocytes and neurons *in situ*. Transmembrane currents evoked in the astrocytes (glial synaptic currents; GSCs in red) and pyramidal neurons (EPSCs, in blue) of layer II/III of mouse neocortex *in situ* by stimulation of neuronal afferents were recorded in presence of 100 μM picrotoxin, 50 μM CNQX and 30 μM PPADS.

A, left panel shows the changes in the amplitude of astrocytic GSCs (red) and neuronal EPSCs (blue) following the bath application of 3 μM UBP141 and 10 μM ifenprodil. Data are presented as mean±SD for 9 cells. ***B***, changes in the astrocytic GSCs (red) and neuronal EPSCs (blue) after application of 1 and 10 μM of memantine (mean±SD for 8 cells). Data shown in the panels ***A*** and ***B*** were measured in constant presence of glutamate transporters antagonists TFB-TBOA, 1 μM and DL-TBOA, 30 μM. Each point in the time graphs shows the average amplitude (relative to control) of 5 sequential currents. Illustrative examples of GSCs and EPSCs (average of 5 traces) recorded as indicated, are shown in the right panels. Note the different inhibitory effects produced by UBP141, ifenprodil and memantine in the astrocytes and neurons.

C, left panel shows the changes in the amplitude of astrocytic GSCs measured immediately after establishing whole-cell recording using intracellular solution supplemented with 10μM MK-801 (mean±SD for 6 cells). D-AP5, UBP141 and combination of TFB-TBOA (1 μM) and DL-TBOA(30 μM) were applied to cortical slices as indicated. Note that UPB141 did not decrease the amplitude of GSCs, when astrocytic NMDA receptors were inhibited by intracellular MK-801, confirming that its action shown in panel A was due to inhibition of glial NMDA receptors.

Figure 4.

Voltage-dependence of the currents mediated by NMDA receptors in astrocytes and neurons.

The upper panels show currents induced by rapid application of NMDA (50 μM, 1 s) recorded at the different holding potentials in a cortical astrocyte (A) and pyramidal neuron (B) in 2 and 20 mM extracellular Ca^{2+} . The lower panels shows the *I–V* curves constructed from 11 (astrocytes) and 6 (neurons) independent experiments. The amplitudes of responses to NMDA were normalized to the value measured at -40 mV; data are presented as mean±SD. Solid lines show the results of a best polynomial fit (least squares routine), intersection with zero current axis gives the following values of reversal potential in 2 and 20 mM Ca^{2+}_{OUT}: 0.92 mV and 7.5 mV for astrocytes and 2.75 and 14.1 mV for neurons. The permeability ratio P_{Ca}/P_{Na} calculated in the framework of extended Goldman-Hodgkin-Katz equation is 3.4 for astrocytes and 7.5 for neurons.

Figure 5

NMDA receptor-mediated Ca^{2+}-signalling in cortical astrocytes.

A, An acutely isolated astrocyte was loaded with Fluo-3 via a somatic patch pipette. Fluorescent images were recorded simultaneously with transmembrane currents evoked by application of 20 μM NMDA and 100 μM glutamate in control and after consecutive application of 30 μM D-AP5. Representative images (left) and glial currents (right, upper row) were recorded before (rest) and after application of agonist. Ca^{2+}-transients (right, lower row) represent the $\Delta F/F_0$ ratio averaged over the cell soma; scale bar is 10μm. Holding potential is -80 mV. Transmembrane current activated by glutamate in control is mediated by NMDA and AMPA receptors and glutamate transporters. The NMDA-component is eliminated by D-AP5. Ca^{2+}-transient activated by glutamate in control is mediated by metabotropic glutamate receptors, NMDA receptors and possibly by Ca^{2+}-permeable AMPA receptors. The Ca^{2+}-transient activated by glutamate in presence of D-AP5 lacks the NMDA-receptor mediated component. **B,** Pooled data (mean±SD for 5 astrocytes) of peak Ca^{2+}-transients; the difference is statistically significant with (*) $P<0.01$ and (**) $P<0.005$ (one-way ANOVA).

Note the significant contribution made by the NMDA receptors to glutamatergic Ca^{2+}-signal in the astrocytes.

Figure 6

Action of glycine and D-serine on astroglial and neuronal NMDA receptors.

(A, B) Representative responses activated in acutely-isolated cortical astrocyte and neuron by consecutive application of 50 μM NMDA (no glycine added), 10 μM glycine, 10 μM D-serine and 20μM NMDA and D-serine together.

(C) Pooled data (mean ± SD for 10 astrocytes and 7 neurons) of amplitude of current activated by glycine, D-serine and NMDA and D-serine together; amplitudes were normalized to the amplitude of NMDA-activated current. Recordings were made at a holding potential of -80 mV in the astrocytes and -40 mV in the neurons.

Note the weak agonist action of glycine and D-serine in the astrocytes.

Figure 7

Action of NMDA receptors antagonists on glycine and D-serine-activated currents in astrocytes.

(A) Representative responses activated in acutely-isolated cortical astrocyte by consecutive application of 50 μM NMDA (no glycine added) and 10 μM glycine in control and presence of 10 μM MK801. NMDA and glycine were applied in turn with 2 min interval. The gradual decline of astrocytic response is indicative of use-depended block; block by MK801 established after 4^{th} -5^{th} round of application. Note the synchronous decrease in the amplitude of both NMDA and glycine-activated currents.

(B) Representative responses activated in acutely-isolated cortical astrocyte by consecutive application of 50 μM NMDA (no glycine added) and 10 μM D-serine in control and after application of 10 μM memantine. NMDA and D-serine were applied in turn with 2 min interval.

(C) Pooled data (mean ± SD for 5 astrocytes) on the inhibitory effect of MK801, memantine and UBP141 on astrocytic responses. Although glycine-activated currents exhibited less sensitivity to antagonists than NMDA-activated currents, the difference was not statistically significant.

All recordings were made at a holding potential of -80 mV in presence of picrotoxin and strychnine.

.

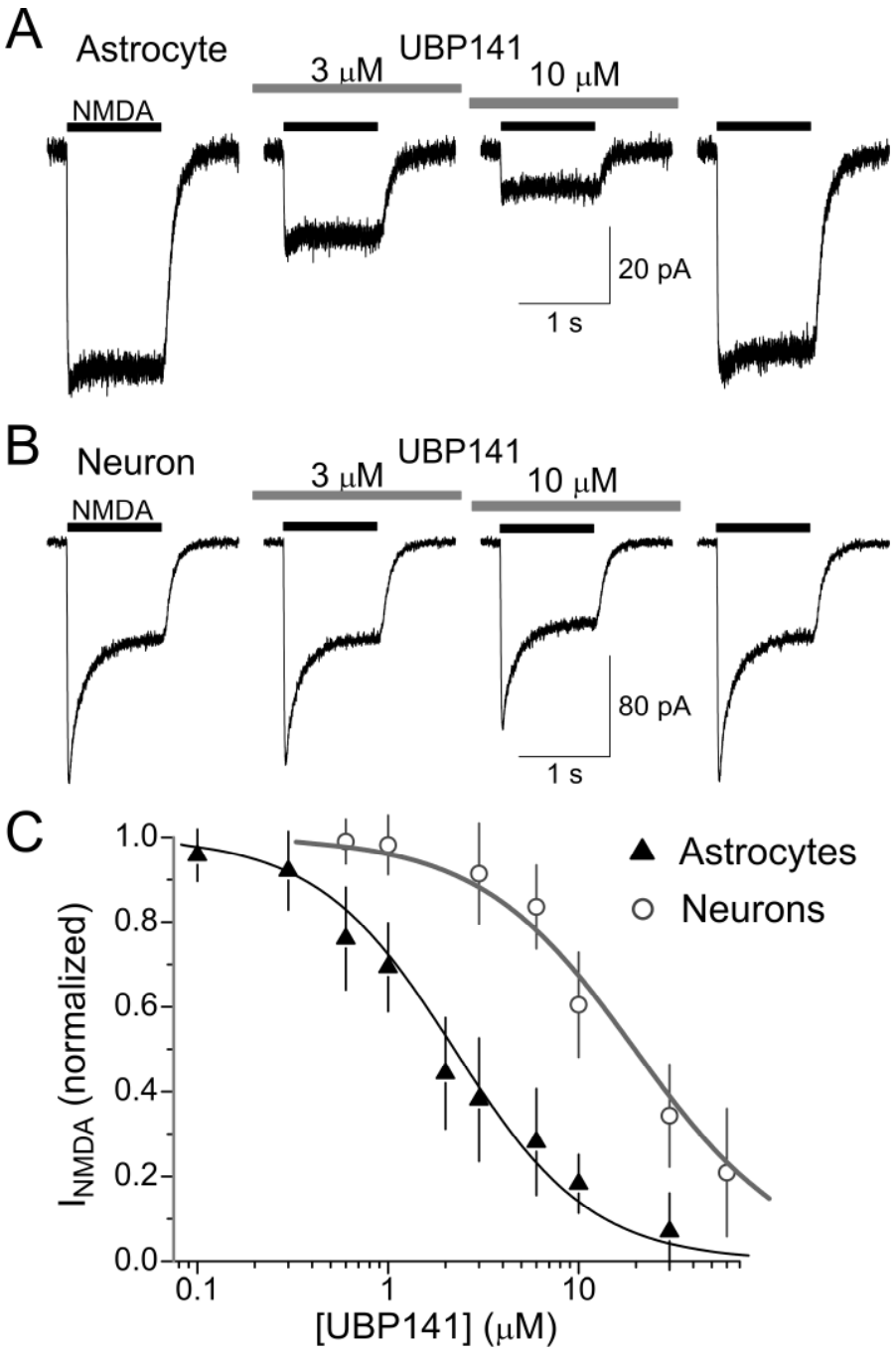
A
Astrocyte
UBP141
3 μM
10 μM
NMDA
20 pA
1 s
B
Neuron
UBP141
3 μM
10 μM
NMDA
80 pA
1 s
C
Astrocytes
Neurons
I_{NMDA} (normalized)
1.0
0.8
0.6
0.4
0.2
0.0
0.1
1
10
[UBP141] (μM)

Fig.1

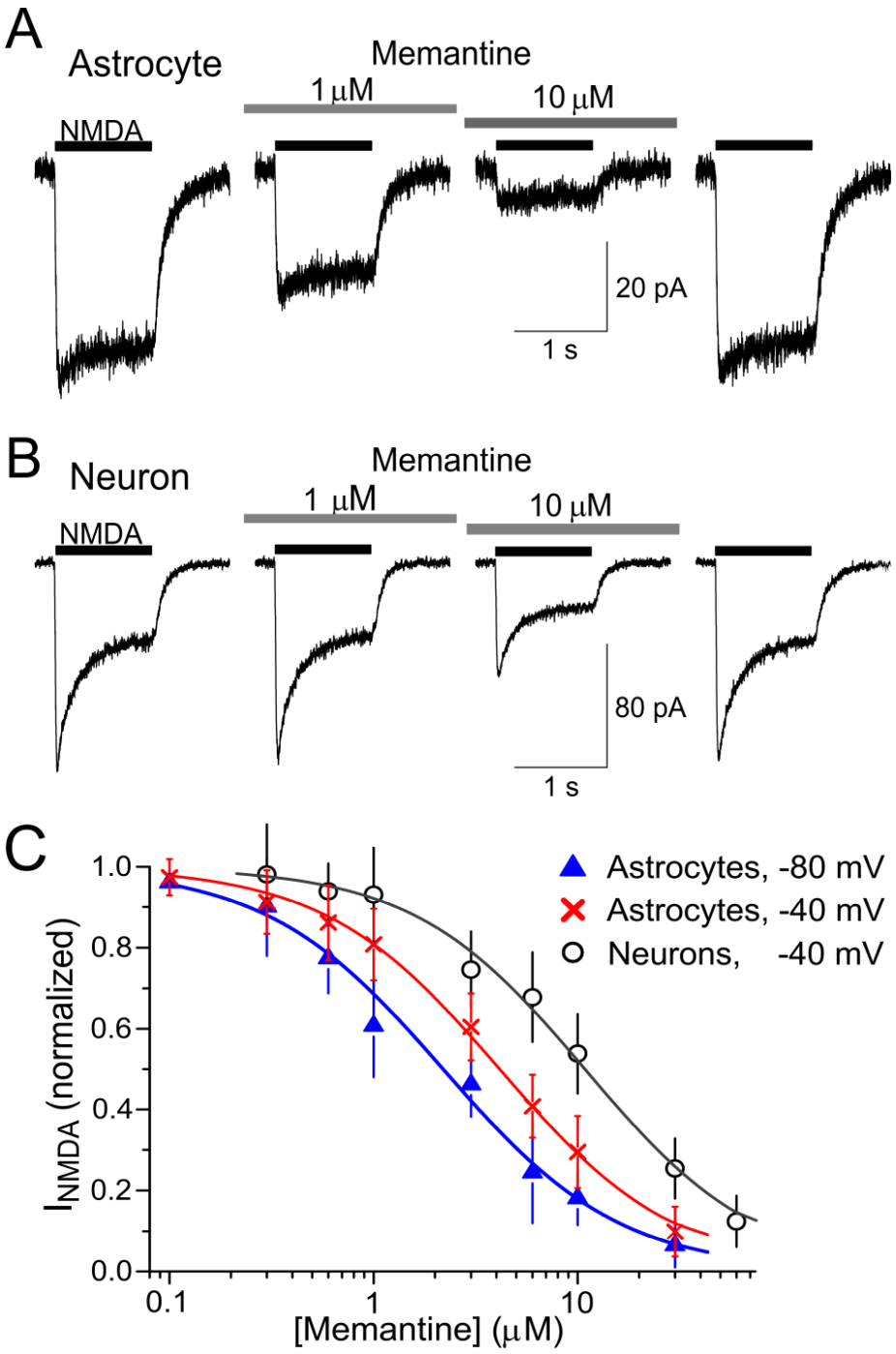
A
Astrocyte
Memantine
1 μM
10 μM
NMDA
20 pA
1 s
B
Neuron
Memantine
1 μM
10 μM
NMDA
80 pA
1 s
C
Astrocytes, -80 mV
Astrocytes, -40 mV
Neurons, -40 mV
I_NMDA (normalized)
1.0
0.8
0.6
0.4
0.2
0.0
0.1
1
10
[Memantine] (μM)

Fig.2

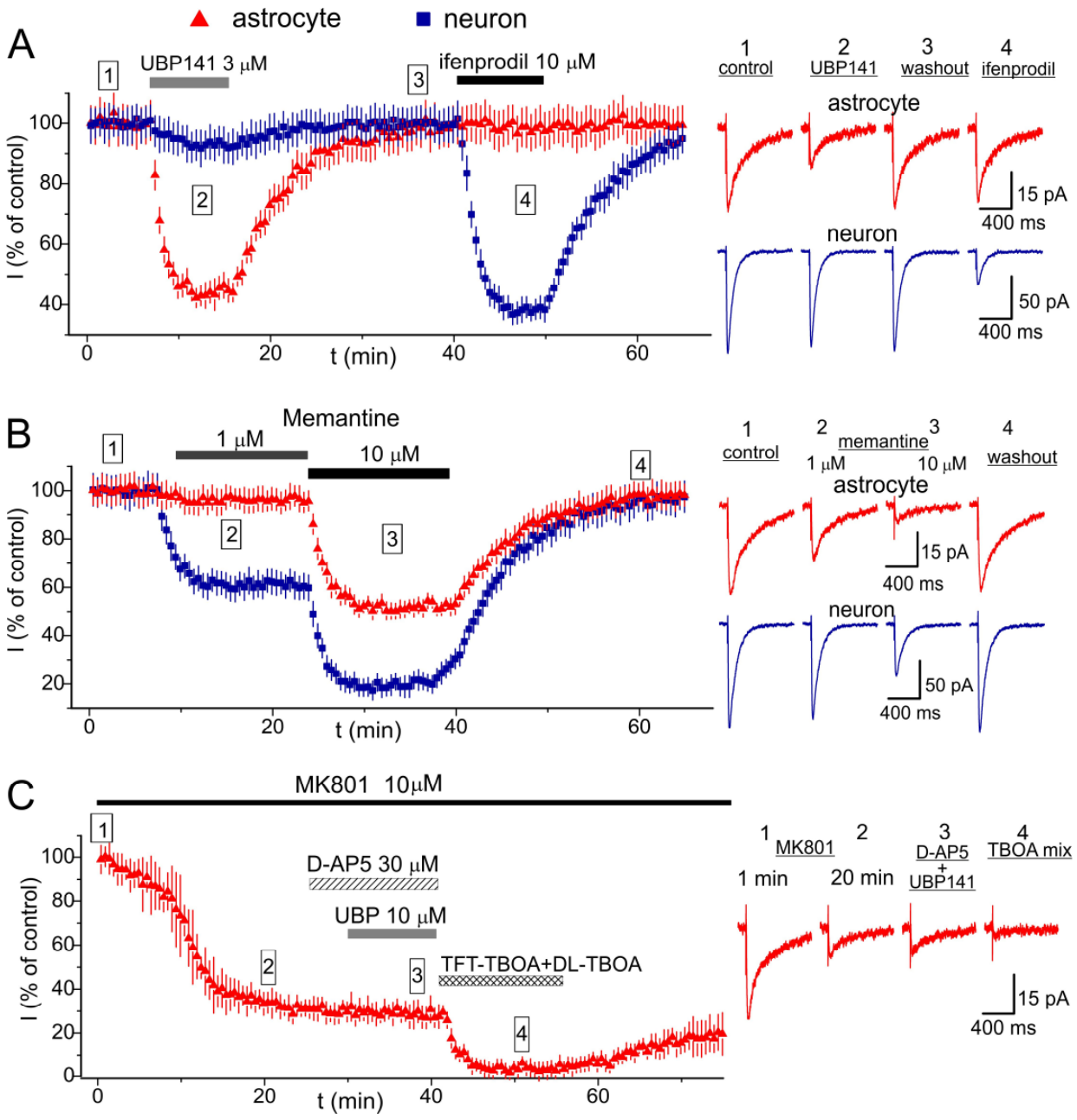
A
astrocyte
neuron
UBP141 3 μM
ifenprodil 10 μM
I (% of control)
t (min)
1 control
2 UBP141
3 washout
4 ifenprodil
15 pA
400 ms
50 pA
400 ms
B
Memantine
1 μM
10 μM
memantine
1 μM
10 μM
washout
C
MK801 10μM
D-AP5 30 μM
UBP 10 μM
TFT-TBOA+DL-TBOA
1 min
20 min
D-AP5 + UBP141
TBOA mix

Fig.3

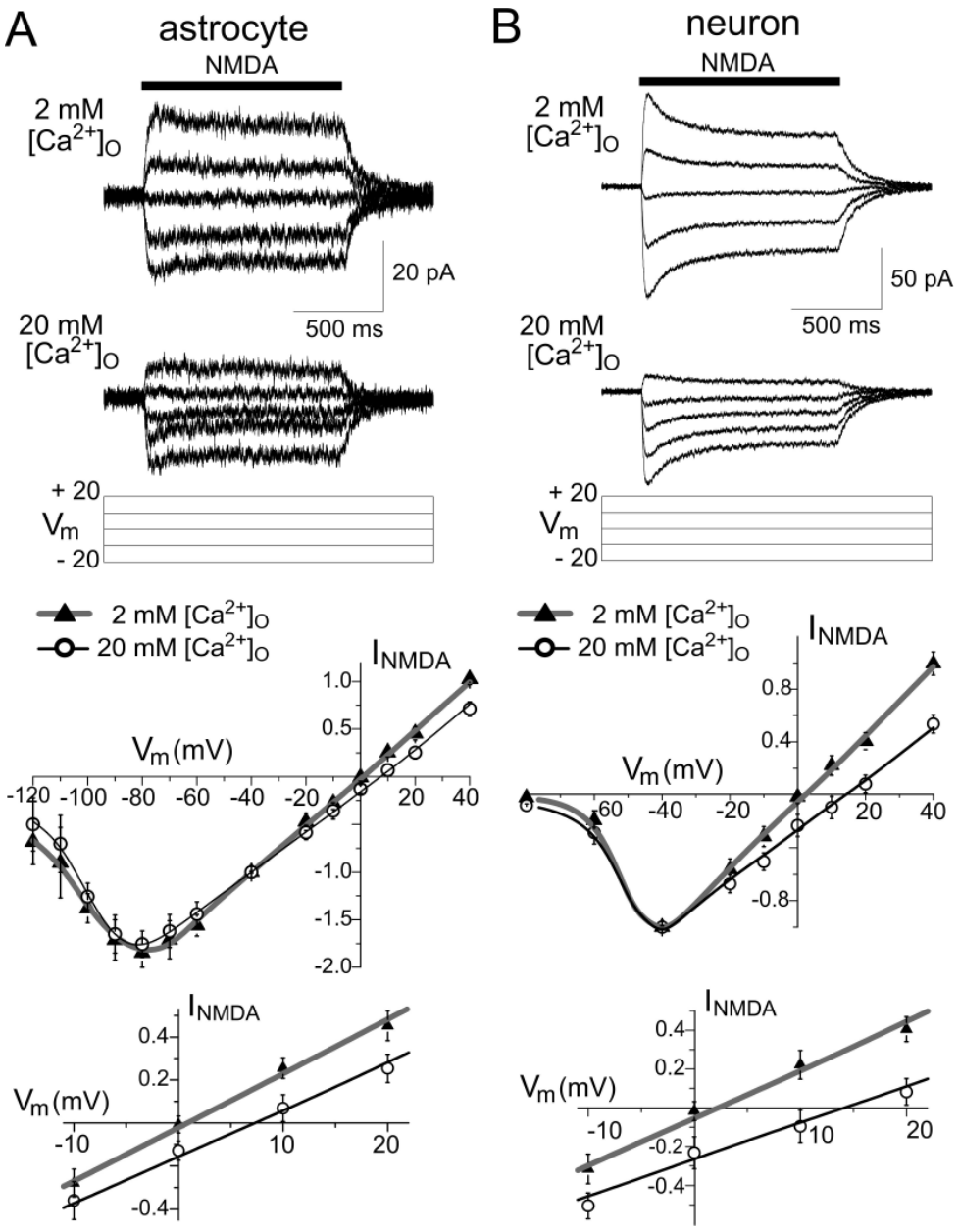
A
astrocyte
NMDA
2 mM [Ca2+]O
20 pA
500 ms
20 mM [Ca2+]O
+ 20
Vm
- 20
2 mM [Ca2+]O
20 mM [Ca2+]O
INMDA
Vm(mV)
1.0
0.5
-120 -100 -80 -60 -40 -20 20 40
-1.0
-1.5
-2.0
INMDA
0.4
0.2
Vm(mV)
-10
10
20
-0.4
B
neuron
NMDA
2 mM [Ca2+]O
50 pA
500 ms
20 mM [Ca2+]O
+ 20
Vm
- 20
2 mM [Ca2+]O
20 mM [Ca2+]O
INMDA
0.8
0.4
Vm(mV)
60 -40 -20 20 40
-0.8
INMDA
0.4
0.2
Vm(mV)
-10
10
20
-0.2
-0.4

Fig.4

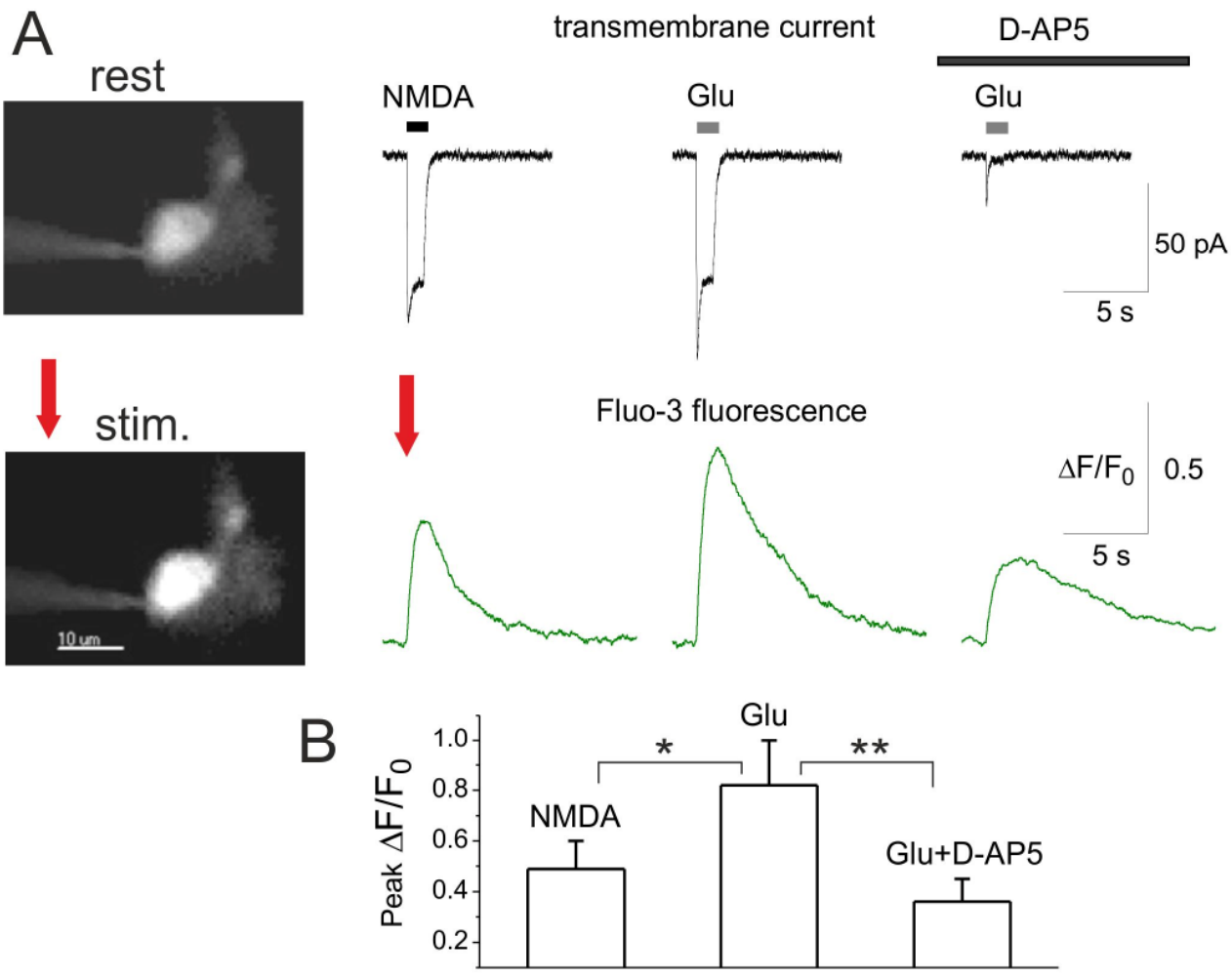
A
rest
stim.
10 um
transmembrane current
D-AP5
NMDA
Glu
Glu
50 pA
5 s
Fluo-3 fluorescence
ΔF/F0
0.5
5 s
B
Peak ΔF/F0
1.0
0.8
0.6
0.4
0.2
NMDA
Glu
Glu+D-AP5
*
**

Fig.5

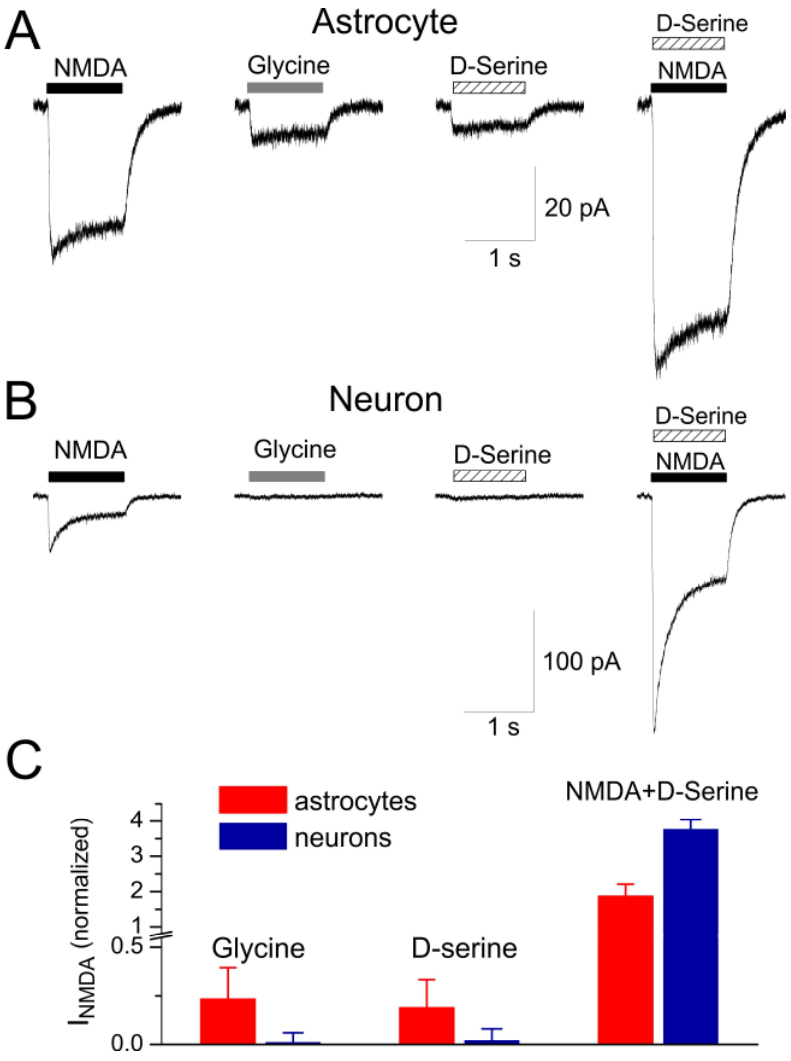
A
Astrocyte
NMDA
Glycine
D-Serine
D-Serine
NMDA
20 pA
1 s
B
Neuron
NMDA
Glycine
D-Serine
D-Serine
NMDA
100 pA
1 s
C
astrocytes
neurons
NMDA+D-Serine
I_{NMDA} (normalized)
4
3
2
1
0.5
0.0
Glycine
D-serine

Fig. 6

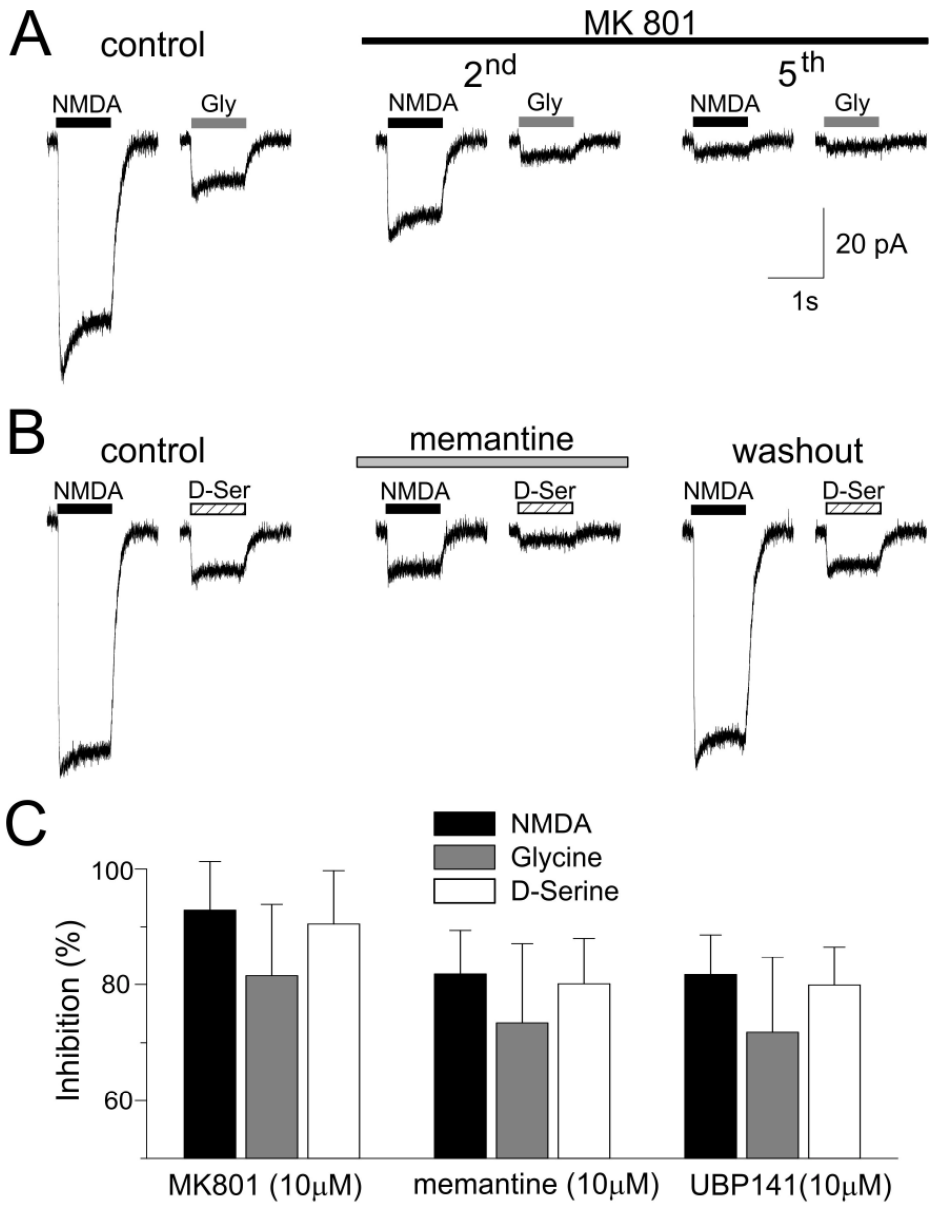
A
control
MK 801
2nd
5th
NMDA
Gly
NMDA
Gly
NMDA
Gly
20 pA
1s
B
control
memantine
washout
NMDA
D-Ser
NMDA
D-Ser
NMDA
D-Ser
C
NMDA
Glycine
D-Serine
100
80
60
Inhibition (%)
MK801 (10μM)
memantine (10μM)
UBP141(10μM)

Fig.7